A semi-mechanistic model for predicting daily variations in species-level live fuel moisture content

Rodrigo Balaguer-Romano [a, b, *], Rubén Díaz-Sierra [a], Miquel De Cáceres [c], Àngel Cunill Camprubí [d], Rachael H. Nolan [e], Matthias M. Boer [e], Jordi Voltas [d, f], Víctor Resco de Dios [d, f, g]

[a] Mathematical and Fluid Physics Department, Faculty of Sciences, Universidad Nacional de Educación a Distancia (UNED), 28040 Madrid, Spain. rodrigo.balaguer.romano@gmail.com (R.B-R.); sierra@ccia.uned.es (R.D-S.)

[b] EIUNED, Escuela Internacional de Doctorado. PhD program in sciences. Universidad Nacional de Educación a Distancia (UNED), 28040 Madrid, Spain.

[c] CREAF, E08193 Bellaterra (Cerdanyola del Vall`es), Catalonia, Spain. miquelcaceres@gmail.com (M. De C.)

[d] Joint Research Unit CTFC – AGROTECNIO – CERCA, Av. Alcalde Rovira Roure 191, 25198 Lleida, Spain. acunill86@gmail.com (A.C.C.)

[e] Hawkesbury Institute for the Environment, Western Sydney University, Locked Bag 1797, Penrith, NSW 2751, Australia. rachael.nolan@westernsydney.edu.au (R.H.N.), M.Boer@westernsydney.edu.au (M.M.B.)

[f] Department of Crop and Forest Sciences, Universitat de Lleida, 25198 Lleida, Spain; jordi.voltas@udl.cat (J.V)

[g] School of Life Science and Engineering, Southwest University of Science and Technology, Mianyang 621010, China. v.rescodedios@gmail.com (V.R. de D.)

* Correspondence: rodrigo.balaguer.romano@gmail.com

Abstract

Live Fuel Moisture Content (LFMC) is one of the main factors affecting forest ignitability as it determines the availability of existing live fuel to burn. Currently, LFMC is monitored through spectral vegetation indices or inferred from meteorological drought indices. While useful, neither approach provides mechanistic insights into species-specific LFMC variation and they are limited in the ability to forecast LFMC under altered future climates. Here, we developed a semi-mechanistic model to predict daily variation in LFMC across woody species from different functional types by adjusting a soil water balance model which estimates predawn leaf water potential (Ψ_{pd}). Our overarching goal was to balance the trade-off between biological realism, which enhances model applicability, and parameterization complexity, which may limit its value within operational settings. After calibration, model predictions were validated against a dataset comprising 1,659 LFMC observations across peninsular Spain, belonging to different functional types and from contrasting climates. The overall goodness of fit for our model (R^2 = 0.5) was better than that obtained by an existing models based on drought indices (R^2 = 0.3) or spectral vegetation indices (R^2 = 0.1). We observed the best predictive performance for seeding shrubs (R^2 = 0.6) followed by trees (R^2 = 0.5) and resprouting shrubs (R^2 = 0.4). Through its relatively simple parameterization, the approach developed here may pave the way for a new generation of process-based models that can be used for operational purposes within fire risk mitigation scenarios.

Key words

Wildfire; Fire behaviour; Drought stress; Drought Code; Remote sensing; Phyrophysiology

Abbreviations

LFMC, Life Fuel Moisture Content; Ψ_{pd}, Predawn leaf water potential; Ψ_{soil}, Soil water potential; DC, Drought Code; EVI, Enhanced Vegetation Index.

1. Introduction

Wildfires are a natural component of many terrestrial ecosystems, but they are becoming an increasing threat to civil protection, public health and national security worldwide (Borchers-Arriagada et al., 2021; Duane et al., 2021; Karavani et al., 2018; McDonald, 2020; Resco de Dios and Nolan, 2021; Tedim et al., 2020). Sustainable wildfire management should not seek to eliminate all fires in ecosystems that are naturally fire-prone. Instead, the target for wildfire management lies in creating fuel structures, from local to landscape scales, that reduce the risk for life and property while maintaining ecological functions. In this context, a key aspect for fire prevention and management actions is understanding the temporal changes that occur in the moisture content of both, dead and live fuels. Wildfires can only occur once critical fuel dryness thresholds are crossed (Jurdao et al., 2012; Luo et al., 2019; Nolan et al., 2016), and management can significantly alter fuel growth and provide a better knowledge of where and when live and dead fuels are in a critically dry state for assessing the risk of large wildfires (Moreno-Gutiérrez et al., 2011).

Wildfire activity depends on the interplay between biomass loads and connectivity along with the availability of such biomass to burn, which is strongly determined by moisture content (Boer et al., 2021). While dead fuel moisture content (DFMC) variations have been far researched (Matthews, 2014), there are significant knowledge gaps regarding live fuel moisture content (LFMC) variations that can be addressed from a plant physiology perspective. LFMC, the water content in live foliage and small twigs on a dry mass basis, critically affects forest ignitability and likelihood of fire spread (Balaguer-Romano et al., 2020; Gabriel et al., 2021; Pimont et al., 2019; Rossa, 2017). This is because the water content of live tissues acts as a heat sink, consequently reducing the intensity of fire and its rate of spread (Rothermel, 1983).

In forest ecosystems, where plant biomass is inherently abundant enough to sustain a fire, fire activity is primarily constrained by the frequency and duration of dry weather periods (Boer et al., 2021). In Mediterranean forests and shrublands, amongst other parts of the world, climate aridity is projected to increase during the 21st century as a result of global change (IPCC, 2021). Consequently, increasing water scarcity may lead to longer fire seasons and higher fire danger as LFMC distributions shift towards drier levels for long periods of time (Ma et al., 2021; Resco de Dios et al., 2021).

Many fire management agencies routinely monitor LFMC directly through time-consuming and expensive field inventories or indirectly through remote sensing products or meteorological drought indices. Remotely-sensed approaches, which include spectral vegetation indices and radiative transfer models, allow the monitoring of LFMC over large areas at fine spatial and temporal resolutions (Yebra et al., 2013). Drought indices, such as the Drought Code (DC) from the Canadian Forest Fire Weather Index (Van Wagner, 1974), are based on daily air temperature and precipitation data and are designed to conceptually represent water dynamics in soil reservoirs. Common limitations to both indirect approaches are that they provide incomplete information on interspecific differences, at least without a priori calibrations, and that forecasting relies on empirical methods. Furthermore, a number of studies have cast doubt on the reliability of DC as an actual proxy of LFMC, at least in some plant functional types in the Mediterranean basin (Ruffault et al., 2018; Soler Martin et al., 2017).

The degree of variation in LFMC within a fire season varies markedly across life-forms, at least in Mediterranean environments (Resco de Dios, 2020). This variation arises from differences in physiological and anatomical characteristics controlling LFMC such as stomatal control, the degree of sclerophylly, or rooting depth (Sánchez-Martínez et al., 2020). Empirical studies have often observed how seasonal variation in LFMC is

largest in seeding shrubs, intermediate in resprouting shrubs and lowest in trees (Nolan et al., 2018; Pellizzaro et al., 2007b; Viegas et al., 2001). Seeding shrubs often have shallow root systems which cannot reach deeper water sources (Nolan et al., 2018), high resistance to embolism (Pausas et al., 2016) and poor stomatal controls (Resco de Dios, 2020), which jointly lead to the lowest LFMC values during drought periods and the largest seasonal variation. Resprouting shrub species often have deeper roots and lower drought tolerance than seeders, leading to intermediate variation in LFMC (Resco de Dios, 2020). Tree species often have the deepest rooting systems and strong stomatal controls, which buffers against short term fluctuations in shallow water levels and, consequently, they often display nearly constant LFMC throughout the fire season (Nolan et al., 2018; Viegas et al., 2001).

Nolan et al. (2020) demonstrated that inter-species variation in LFMC could in principle be modelled as a function of predawn leaf water potential (Ψ_{pd}), given information on pressure-volume relationships. This approach can be further simplified and LFMC may be modelled from Ψ_{pd} using solely a linear regression when plants are operating below the turgor loss point, which is the most critical from the perspective of fire occurrence (Nolan et al., 2018). In a case study using six species from a Mediterranean forest, the prediction of LFMC from Ψ_{pd} showed an overall goodness of fit that was better than that from existing drought indices (Nolan et al., 2018). To scale up from local to larger areas, LFMC predictions would require predictions of Ψ_{pd} which, in turn, is strongly related to rhizosphere soil water potential (Ψ_{soil}). That is, Ψ_{pd} overnight equilibrates with Ψ_{soil} in the absence of nocturnal transpiration or significant disruptions in the soil-plant-atmosphere continuum (Ritchie and Hinckley, 1975). However, to our knowledge, no study has yet attempted large scale LFMC modelling by coupling a soil water balance model with a physiological model.

MEDFATE is a forest ecosystem model designed to simulate soil and plant water balances in forest stands with heterogeneous structure and composition (De Cáceres et al., 2021, 2015). Aboveground stand structure is represented by total height, leaf area index and crown ratio of a set plant cohort. In MEDFATE, a plant cohort represents a set of plants that belong to the same species with similar structural characteristics, including root distribution, which is specified using the depths corresponding to cumulative 50% and 95% of fine roots. Soil is represented using a set of vertical layers with different depths and physical properties. Finally, the model requires daily weather data as inputs to simulate plant hydraulics and transpiration at subdaily time steps (De Cáceres et al., 2015).

Here we seek to develop a novel approach for forecasting daily variations in LFMC across Mediterranean species by merging soil and plant water potential simulations from MEDFATE (De Cáceres et al., 2021) with previously developed Ψ_{pd}-LFMC based models (Nolan et al., 2018). More specifically, we seek to model LFMC variation across species grouped in three functional types (seeding shrubs, resprouting shrubs and trees) from Ψ_{pd} values, and compare the results with current approaches such as the Drought Code and remotely sensed vegetation indices. To this end, we used the Spanish subset of a global LFMC database (Yebra et al., 2019) for calibration and validation. Our ultimate goal was to develop an approach that can be used within operational settings. Considering the usual trade-off between the degree of biological realism that is incorporated into a model and how applicable and easy to use the model will be, we seek to merge simplicity with biological realism to enhance applicability by making some simplifying assumptions on the biological differences across species.

2. Materials and Methods

2.1 Globe-LFMC database

Globe-LFMC is a global database of live fuel moisture content measured from 1,383 sampling sites in 11 countries (Yebra et al., 2019). Each individual record represents an *in situ* destructive measurement of LFMC. We selected all sites within Spain with species specific records, resulting in 40 sampling sites containing 2,511 individual records with observed LFMC. Data includes 37 species (Methods A1) from 21 different genera covering a sampling period of 20 years from 1996 to 2017 (Table A1). Sampling sites cover many of the contrasting climates and ecoregions of peninsular Spain (Fig. 1).

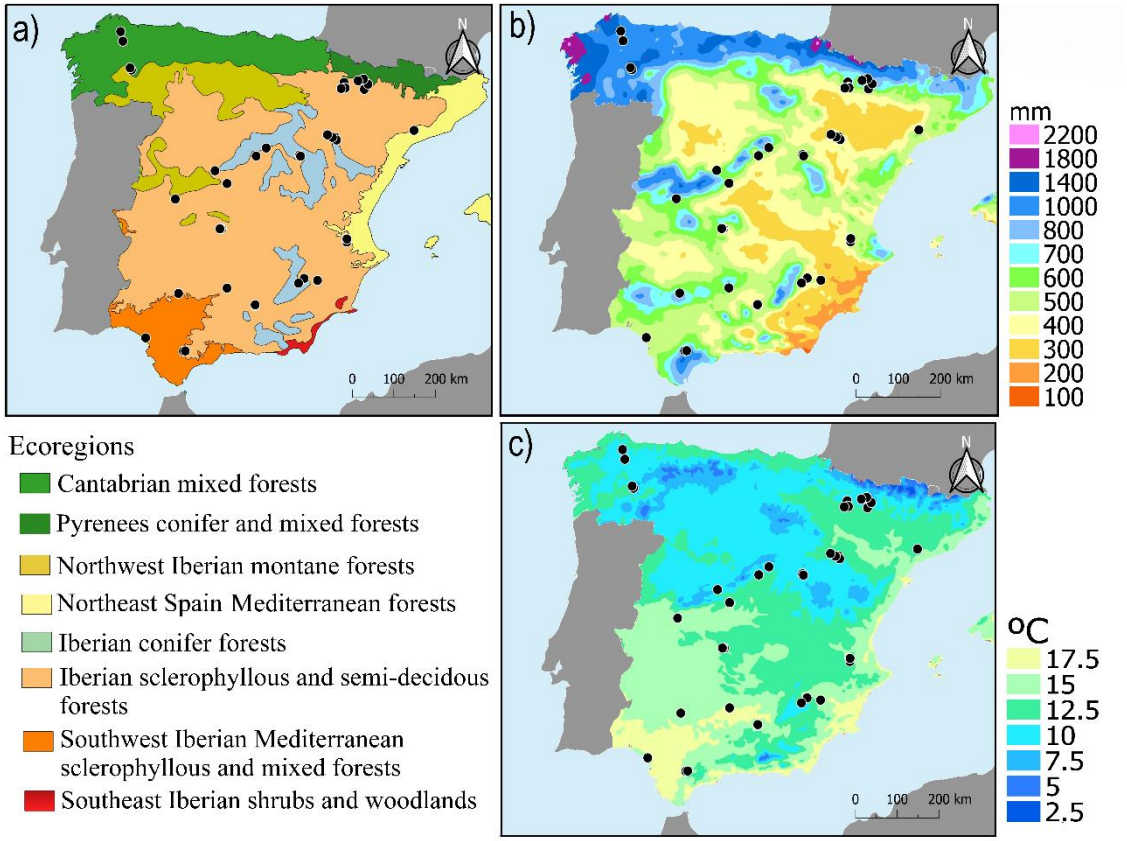

Figure 1. Globe-LFMC sampling sites in Spain. a) Ecoregions, b) mean annual precipitation and c) mean annual air temperature. Black circles indicate the location of our study sites. Ecoregions delimitations obtained from (Dinerstein et al., 2017) and meteorological gradients from (Chazarra Bernabé et al., 2018).

Mean annual air temperature varied from 10.9 to 17.8ºC and mean annual precipitation from 243 to 1,345 mm across the selected sampling sites (Fig. 1.b-c, Table

A1). Vegetation types and ecoregions ranged from xeric sclerophyll or Mediterranean pine forests to the more mesic Cantabrian mixed forests, dominated by temperate deciduous broad-leaf species (Fig. 1.a).

2.2 MEDFATE

MEDFATE (version 2.2.3) is a process-based soil-vegetation-atmosphere transfer model implemented in an R package, which uses soil, vegetation, and meteorological data to predict soil moisture dynamics (De Cáceres et al., 2021; Table A2). The model is based on the BILJOU and SIERRA water balance models (Granier et al., 1999; Mouillot et al., 2001) and predicts, at a daily time steps, the soil water content as a function of soil properties, stand structure and daily climatic variables. Thus, daily changes in soil water content are calculated as the difference between precipitation, the water input, and canopy interception, plant transpiration, bare soil evaporation, surface runoff and deep drainage (De Cáceres et al., 2021, 2015). Also, the model predicts daily plant transpiration and photosynthesis rates. Based on Sperry et al. (2017), stomatal regulation of gas exchange is simulated at sub-daily steps involving detailed calculations of hydraulics, leaf energy balance and photosynthesis.

We divided the soil into four layers (0-10 cm, 10-20 cm, 20-60 cm and 60-100 cm deep). When a given soil layer is filled, water percolates to the next layer below, except in the deepest layer where water is lost from the profile via deep drainage. Soil data inputs are bulk density, the percentage of clay, sand, organic matter and rock fragment content, which were derived from the Soil Grids System at 250 m resolution (Hengl et al., 2017). A previous sensitivity analysis has shown that modelled transpiration is more sensitive to meteorological or vegetation inputs such as annual rainfall and leaf area index (LAI) than to soil inputs such as soil depth of layers or soil texture variation from clayey soils to sandy soils (De Cáceres et al., 2015).

Vegetation data inputs are species identity, tree density, shrub cover, plant height, tree diameter at breast height and plant rooting depth. All data except rooting depth were obtained from the nearest plot which includes the target species from the Third National Forest Inventory of Spain (Alberdi et al., 2016), following the same approach as in previous publications (De Cáceres et al., 2021). MEDFATE requires the rooting depth where the cumulative 50% (Z50) and 95% (Z95) of fine roots occur. Previous studies have incorporated species-specific differences from a model assuming that vegetation is at eco-hydrological equilibrium (Cabon et al., 2018). However, to simplify model parameterization and diminish computational demands, we assumed that Z50 and Z95 occurred at 10 cm and 20 cm for seeding shrubs (R-), at 20 cm and 75 cm for resprouting shrubs (R+) and at 20 cm and 100 cm for trees (Tr), respectively. We chose these depths as they are consistent with previously defined soil depths and with our assumptions that seeding shrubs (R-) have shallow root systems that can only access shallow water resources; that tree (Tr) species have the deepest rooting systems and are able to extract water from superficial and also from deep layers; and that resprouting shrubs (R+) have an intermediate root distribution. MEDFATE also includes a set of species-specific plant traits covering plant size, shrub and tree allometric coefficients to predict biomass fuel loading, phenology and anatomy characteristics, tissue moisture, light extinction, transpiration, and photosynthesis (De Cáceres et al., 2021). We used the default values for each species with the aim of using a parsimonious parameterisation to enhance the potential application of the model.

Temperature, precipitation and wind speed were obtained for each sampling site (in a 0.1º x 0.1º grid) from the ERA-5 Land reanalysis dataset (Hersbach et al., 2020), which provides hourly estimates of climate variables from the Copernicus Climate Change Service. Daily meteorological variables of relative humidity, incoming solar

radiation, and potential evapotranspiration were then obtained using the *meteoland* R package (De Cáceres et al., 2018). Relative humidity was estimated assuming that dew point temperature equals the minimum temperature, and potential solar radiation was estimated from latitude, slope and aspect. Incoming solar radiation was then obtained following Thornton and Running (1999).

Input data were then used to predict daily species-specific Ψ_{pd} values and simulations were ran with a one-year spin-up period to avoid interferences from initial conditions.

2.3 Model calibration and validation

We divided the Globe-LFMC database into a calibration and a validation dataset. The calibration dataset was obtained by randomly sampling among sites and species using 34 % of the total dataset, that is, 852 data points. After obtaining Ψ_{pd} from MEDFATE, we calibrated its relationship with LFMC based on a linear regression where, following Nolan et al., (2018), Ψ_{pd} had been logarithmically transformed. We used a single relationship between LFMC and Ψ_{pd} for all species in the entire dataset, instead of using separate relationships for each species. This is because we sought to increase model simplicity within operational settings and because not all the species present in the dataset had enough measurements for independent calibration. The validation dataset, containing the remaining 1,659 data points (representing 66% of the total), was used to validate the LFMC predictions. Model validation was performed by a linear regression between observed and predicted LFMC calculating the adjusted R-squared (R^2) to measure the goodness of fit of our predictions, as well as the intercept (β_0) and the slope (β_1), and their 95% confidence interval, to test for model prediction biases. We also calculated the root mean square error (RMSE) and the mean absolute error (MAE) to quantify the accuracy

of the predictions, and the mean biased error (MBE; Jolliff et al., 2009) to assess if our predictions underpredict or overpredict observed data.

2.4 Drought Indices and Spectral Vegetation Indices

We compared the goodness of fit of our approach with predictions from existing drought indices and spectral vegetation indices using the same Globe-LFMC database validation dataset. We obtained Drought Code (DC) values using the Canadian Forest Fire Danger Rating System, as implemented in the *cffdrs* R package (Wang et al., 2017), using the same meteorological data sources as those previously described for MEDFATE, and also leaving a one year spin-up period to avoid interference from initial conditions.

Following Marino et al. (2020), we calculated nine spectral indices (Table A3) to infer LFMC using data from the Moderate Resolution Imaging Spectrometer (MODIS) MCD43A4 Collection 6 reflectance product produced acquired daily tiles at 500-meter resolution. Data was downloaded from the NASA Land Processes Distributed Active Archive Center (LP DAAC, https://lpdaac.usgs.gov/). Then, for each sampling date and site we extracted the values of each MODIS band as a simple pixel extraction which corresponded with the sampling site area. We regressed the spectral indices against observed LFMC to select the index with the highest adjusted R^2 in subsequent analyses (Enhanced Vegetation Index (EVI), R^2=0.33, Fig. A1). As EVI values included all the species present in the sampling site area, we additionally calculated the equivalent water thickness (*EWT*) from individual LFMC values to enhance comparability. EWT, which is a measure of water content per unit surface area of the vegetation (Sow et al., 2013), was calculated following Chakroun et al. (2015):

$$EWT = \frac{1}{\rho_w}\frac{1}{N}\sum(LFMC_i)\left(\frac{1}{SLA_i}\right) \quad (1)$$

where LFMC is the observed foliar moisture content recorded in the Globe-LFMC database, ρ_w is the density of pure water (1000 kg m^{-3}) and SLA is the specific leaf area. Species-specific SLA values were obtained from the MEDFATE plant traits set. We calculated the *EWT* of N species contained in each study site for each sampling date by applying equation (1) for *i* species. Finally, as vegetation index signals saturate in the upper ranges, *EVI* values were logarithmically transformed before regression against EWT.

2.5 Statistical analysis

To assess for significant differences across the approaches used for calibration, we used an encompassing test of Davidson and MacKinnon (1993) with the "*lmtest*" R package (Zeileis and Hothorn, 2002). To compare two non-nested models, the test fits a third encompassing model which contains all regressors from both models. Then, the *encomptest()* function performs a Wald test for comparing each models against the encompassing model. If there are significative differences between each linear model against the encompassing model, the test indicates that both linear models are significantly different.

3. Results

The dataset allowed for model testing and calibration under a wide range of LFMC values, which varied across functional groups as expected. That is, LFMC variation was largest in seeding shrubs (45-145%, 5 and 95% percentiles, respectively), and intermediate in resprouting shrubs (60-120%). Average variations in trees (75-140%) were larger than in shrubs due to physiological differences between *Pinus* and *Quercus*, although seasonal variations within each genus were smaller than those obtained for seeders and resprouters. Across all species and years, the average seasonal values varied between 125% in spring to 80% in summer.

288

289 3.1 Calibration, validation and comparison of *MEDFATE*, *DC* and *EVI.*

290 Using the calibration dataset, we regressed predicted Ψ_{pd} (logarithmically transformed),
291 and DC values against observed LFMC, and EVI (logarithmically transformed) against
292 the equivalent water thickness (EWT) (Fig. A2). The encompassing test of Davidson and
293 MacKinnon showed significant differences ($p < 0.001$) in the predictions of LFMC based
294 on MEDFATE and on DC, against the encompassing model which contains all regressors
295 from both models. Our model showed significantly better fit than DC (Fig. A2). EVI
296 could not be included in this analysis as the response variables were different (LFMC vs
297 EWT). Then, the equations derived from these linear regressions were subsequently
298 applied to Ψ_{pd}, DC and *EVI* values obtained for the validation dataset. LFMC predictions
299 using our approach ($MEDFATE_{LFMC}$) showed a substantial improvement over those based
300 on the drought index (DC_{LFMC}) and the spectral vegetation (EVI_{EWT}) index (Table 1, Fig.
301 2).

302 **Table 1.** Goodness of fit statistics for the three approaches used in this study: $MEDFATE_{LFMC}$, Drought Code
303 (DC_{LFMC}) used to predict LFMC, and Enhanced Vegetation Index (EVI_{EWT}) used to predict EWT, for each
304 functional type (R-, seeding shrubs; R+, resprouting shrubs; Tr, trees). We calculated the adjusted R-
305 squared (R^2), the intercept (β_0), and the slope (β_1), with each standard error in brackets, of the regression
306 between observed and predicted LFMC, and also the root mean square error (RMSE), mean absolute error
307 (MAE) and mean biased error (MBE) and the 95% confidence interval for correlation coefficients (CI_{low} and
308 CI_{up}).

	R^2	β_0	β_1	*RMSE*	*MAE*	*MBE*	CI_{low}	CI_{up}
$MEDFATE_{LFMC}$	0.5	-25.4 (±3.1)	1.4 (±0.0)	31.1	22.3	-8.8	1.3	1.4
R-	0.6	-28.9 (±3.4)	1.4 (±0.0)	28.7	21.5	-4.8	1.3	1.4
R+	0.4	-22.1 (±12.1)	1.4 (±0.1)	32.4	21.4	-12.9	1.1	1.6
Tr	0.5	-22.7 (±7.7)	1.4 (±0.1)	34.7	22.7	-15.8	1.2	1.6
DC_{LFMC}	0.3	-6.2 (±3.7)	1.1 (±0.0)	33.6	24.3	-3.4	1.0	1.2
R-	0.5	-46.7 (±4.3)	1.5 (±0.0)	31.3	23.4	-4.6	1.5	1.6
R+	0.07	49.5 (±5.9)	0.4 (±0.1)	31.2	22.5	6.5	0.3	0.5
Tr	0.09	44.2 (±11.1)	0.7 (±0.1)	41.6	29.5	-14.6	0.5	1.0

EVI_{EWT}	0.1	-0.001(±0.0)	1.0 (±0.0)	0.005	0.003	-0.0002	0.9	1.2
R-	0.1	0.001 (±0.0)	0.7 (±0.0)	0.002	0.001	0.0004	0.6	0.9
R+	0.2	-0.001 (±0.0)	0.9 (±0.1)	0.004	0.003	0.0004	0.8	1.3
Tr	0.03	-0.004 (±0.0)	0.9 (±0.4)	0.01	0.008	-0.0002	0.4	1.4

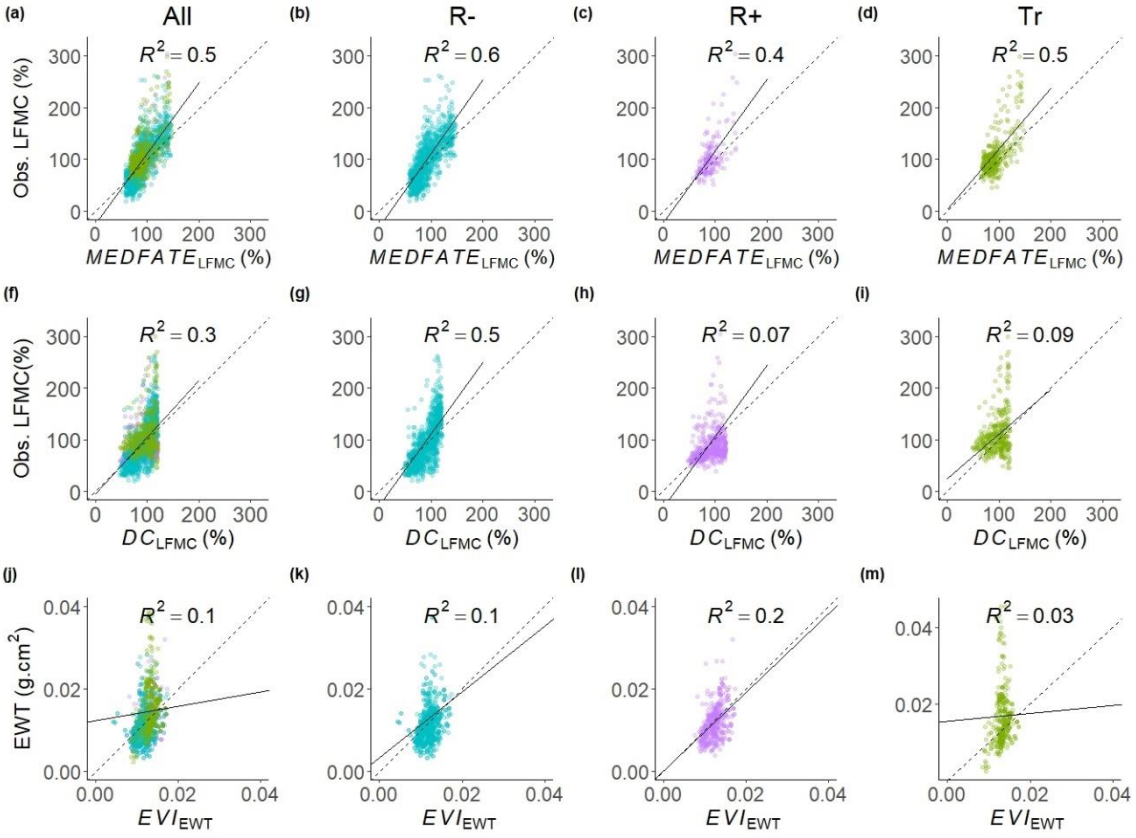

Figure 2. Observed LFMC against predicted values from $MEDFATE_{LFMC}$ (a-d) and Drought Code (DC_{LFMC}; f-i), and Equivalent Water Thickness against Enhanced Vegetation Index (EVI_{EWT}; j-m) for all the data (a, f, j) or separately across functional types of seeding shrubs (R-; b, g, k) in blue, resprouting shrubs (R+; c, h, l) in purple and trees (Tr; d, I, m) in green. The line and the R^2 indicate the results of least squares fitting.

The overall goodness of fit of our model, $MEDFATE_{LFMC}$ (R^2 of observed against predicted LFMC relationship of 0.5), was better than for DC_{LFMC} (R^2 = 0.3) or EVI_{EWT} (R^2=0.1). The RMSE and MAE in our model (31 and 22%, respectively) were also smaller than in DC_{LFMC} (34 and 24%, respectively). It is worth noting that the goodness of fit in DC_{LFMC} depended on the functional type. That is, DC_{LFMC} showed a reasonable performance (R^2= 0.5) for seeding shrubs (Fig. 2h), albeit lower than in our model (R^2 = 0.6, Fig. 2c). However, neither DC_{LFMC} nor EVI_{EWT} were reliable predictors of LFMC or

EWT respectively as the coefficients of determination in resprouting shrubs or trees were lower than $R^2 = 0.2$ in all cases (Fig. 2).

3.2 $MEDFATE_{LFMC}$ features.

Despite the improvement of $MEDFATE_{LFMC}$ over DC_{LFMC} and EVI_{EWT}, it is worth noting that our approach tended towards underprediction, particularly in the upper range of LFMC values (Fig. 2, Table 1). We observed that the slope of the observed vs predicted regression was 1.4 and the MBE was -8.8%, indicating this tendency towards underprediction. Our approach showed better goodness of fit for seeding shrubs (R^2= 0.6, MAE =21%) than for trees (R^2= 0.5, MAE =23%) or resprouting shrubs (R^2= 0.4, MAE =21%). Also, we observed that MBE was lower for seeding shrubs (-5%) than for resprouters (-13%) or trees (-16%; Table 1). Predictions of LFMC from $MEDFATE_{LFMC}$ realistically captured the differences in temporal patterns of moisture content (Fig. A3), across genus (Table 2) and species (exemplified in Fig. 3).

Table 2 Goodness of fit statistics for each genus LFMC predicted with $MEDFATE_{LFMC}$. Sample size (n), adjusted R-squared (R^2), intercept (β_0) and slope (β_1), with each standard error in brackets, from regressing observed against predicted LFMC for all the data, and also separately for each functional type and each genus (when n>20). We also show the root mean squared error (RMSE), mean absolute error (MAE), and mean bias error (MBE) and the 95% confidence interval for correlation coefficients (CI_{low} and CI_{up}).

	n	R^2	β_0	β_1	RMSE	MAE	MBE	CI_{low}	CI_{up}
Cistus (R-)	483	0.7	-5.3 (±3.5)	1.1 (±0.0)	20.7	16.1	-5.4	1.0	1.2
Lavandula (R-)	33	0.5	-149.6 (±50.6)	3.0 (±0.6)	68.4	52.9	-34.2	1.9	4.2
Salvia (R-)	473	0.6	-43.2 (±5.3)	1.5 (±0.1)	30.1	24.0	-5.6	1.4	1.6
Thymus (R-)	47	0.7	-251.2 (±31.3)	3.9 (±0.4)	41.8	33.6	4.9	3.2	4.7
Ulex (R-)	46	0.5	-19.4 (±23.1)	1.1 (±0.3)	24.2	20.5	10.7	0.6	1.7
Arbutus (R+)	29	0.5	-24.3 (±37.9)	1.7 (±0.3)	62.1	50.5	-49.1	1.0	2.4
Buxus (R+)	53	0.4	53.4 (±12.5)	0.5 (±0.1)	13.2	11.3	-4.3	0.2	0.7

Erica (R+)	43	0.3	4.5 (±18.1)	0.9 (±0.2)	21.2	17.6	3.4	0.5	1.3
Genista (R+)	30	0.6	-71.1 (±22.7)	1.7 (±0.3)	22.8	19.4	11.8	1.2	2.3
Pinus (Tr)	121	0.5	64.4 (±16.9)	0.4 (±0.2)	20.5	16.8	-7.2	0.1	0.7
Quercus (Tr)	347	0.6	-28.2 (±7.9)	1.5 (±0.1)	36.4	23.1	-17.5	1.3	1.7

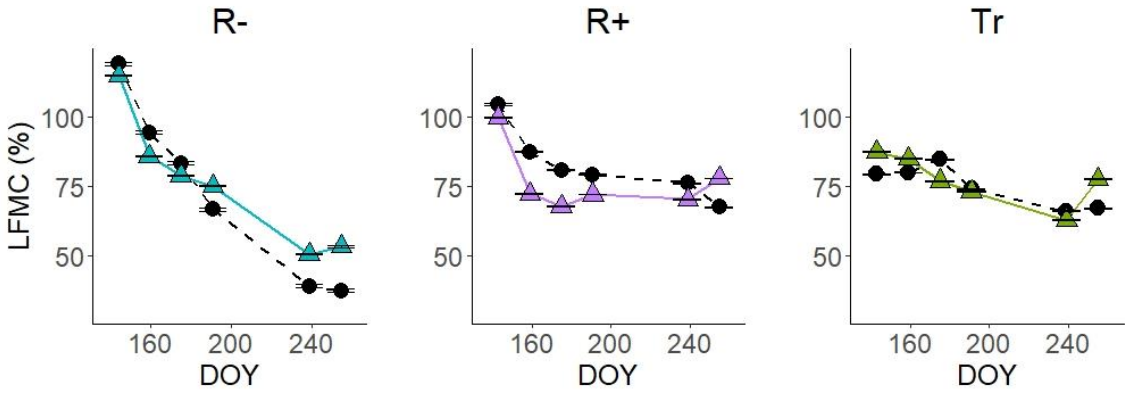

Figure 3. Observed (black dashed line) and *MEDFATE*$_{LFMC}$ predicted (colour continuous line) LFMC seasonal dynamics across functional types, including a seeder (R-, *Genista scorpius*) in blue, a resprouting shrub (R+, *Quercus coccifera*) in purple and a tree (Tr, *Quercus ilex*) in green, in a representative sampling location (*AraCin12*). Error bars indicate standard error.

The performance of the *MEDFATE*$_{LFMC}$ model generally increased when examining variations at the genus level. We observed the best goodness of fit across seeding genera like *Cistus* (R^2 = 0.7, MAE = 16%), *Thymus* (R^2 = 0.7, MAE = 34%), *Salvia* (R^2 = 0.6, MAE = 24%), *Lavandula* (R^2 =0.5, MAE = 53%) and *Ulex* (R^2 =0.5, MAE = 20%). We observed a higher β_1 for *Thymus* (3.9) and *Lavandula* (3.0), indicating stronger underprediction of the model, but the slope remained between 1.1-1.5 for the other seeder shrubs. LFMC predictions for the two tree genera, *Pinus* and *Quercus*, showed an R^2 =0.6 (*Quercus*) and R^2 =0.5 (*Pinus*) and MAE between 37% (*Quercus*) and 17% (*Pinus*). For resprouting shrubs, we observed a larger variation in goodness of fit, as the coefficient of correlation ranged from R^2 = 0.3 in *Erica* (MAE = 18%), to R^2 = 0.5 in *Arbutus* (MAE = 50%), R^2 = 0.5 in *Buxus* (MAE = 11%) and R^2 = 0.6 in *Genista* (MAE = 20%).

4. Discussion

We developed, calibrated and validated a novel approach to predict daily values of LFMC across different species after modelling Ψ_{pd} using a plant-soil water balance model. Our approach keeps a compromise between being mechanistic and operational, as it makes a series of simplifying assumptions on the rooting depth parameters which drive, among others plant traits, inter-specific and seasonal differences. Importantly, we were able to realistically capture seasonal variations (Fig. A3) in LFMC across individuals belonging to different species (Fig. 3), genus (Table 2) and functional types (Fig. 2), and, overall, we demonstrated that our approach had a higher predictive ability than approaches based on remotely sensed spectral vegetation indices or drought indices (Table 1, Fig. 2).

Our *MEDFATE*$_{LFMC}$ model was able to realistically capture the temporal patterns of variation in LFMC across functional types. Following expectations, species with shallower root systems, such as seeding shrubs, showed faster LFMC reductions during the summer dry period (Fig. 3). On the other hand, tree species with deeper root systems were less responsive to seasonal dryness, showing relatively little seasonal variation in LFMC, consistent with their larger dependence on deep soil water pools. Finally, resprouting shrub species show an intermediate dependence on shallow and deep water pools between seeding shrubs and tree species, resulting in an intermediate level of seasonal LFMC variation (Nolan et al., 2018).

We observed a better performance for modelling LFMC in seeding shrubs and trees than for resprouting shrubs. This may be due to a lack of temporal continuity in resprouting shrub records at most sampling sites, as there were only two sites with more than three consecutive weekly measurements. Temporal discontinuity in the data can in turn decrease model performance due to poor data quality (Quan et al., 2021). Another possibility for a poorer model performance in resprouters could be the smaller temporal

388 variation in LFMC records. At any rate, our method for predicting LFMC in resprouters
389 presents a significant improvement over existing commonly used approaches based on
390 optical remote sensing and drought indices (Fig. 2).

391 It is likely that LFMC predictions from our approach could be improved further
392 by a more realistic description of the factors creating temporal variation as well as
393 differences across species. Further studies using our model may derive LFMC from Ψ_{pd}
394 as presented here (Fig. A2), but they are encouraged to develop their own calibration,
395 particularly if dealing with very different vegetation types. Also, it is important that future
396 studies consider the possibility of using species-specific pressure-volume curves to obtain
397 LFMC estimates from Ψ_{pd} (Nolan et al., 2020) to understand whether better predictions
398 may be obtained.

399 LFMC depends on water content relative to dry mass (Pimont et al., 2019),
400 consequently, the incorporation of processes affecting dry mass may lead to further
401 improvements (Jolly et al., 2014). Seasonal changes in specific leaf area, for instance,
402 may alter maximum LFMC (Nolan et al., 2020). Similarly, differences in specific leaf
403 area across species are likely to alter the relationship between LFMC and Ψ_{pd}. That is, at
404 a given water potential (or water content), we can expect higher LFMC in species with
405 larger specific leaf area because dry matter content will be lower. A more realistic
406 description of rooting depth may also be achieved by coupling species-specific root depth
407 models (Cabon et al., 2018). However, we chose not to incorporate these variables in the
408 current study because we sought to develop a relatively simple model that could be easily
409 regionalised to work at national scales within operational settings. Further research could
410 address to which extent model predictions could be improved by incorporating
411 phenological as well as inter-specific differences in dry mass and rooting depth.

412 We observed that DC provided reliable LFMC predictions for seeding shrubs, but
413 not for trees or resprouting shrubs species (Fig. 2). In the case of EVI, we always observed
414 a poor relationship with EWT. LFMC varies over longer time-scales than the period
415 between two consecutive MODIS measurements (Pellizzaro et al., 2007a; Resco de Dios
416 et al., 2021; Viegas et al., 2001). The slight temporal mismatch between LFMC and
417 MODIS measurements is thus unlikely to significantly affect the results. Our goal was to
418 develop a species-specific model, and, to that end, our approach showed a superior
419 performance, allowing, for example, to model understory and overstory species
420 separately, while remotely sensed models typically provide an integrated estimate. It is
421 likely that EVI computed from remotely sensed imagery with higher spatial (i.e., Sentinel
422 3), will show a stronger relationship with species-specific LFMC values than the one
423 shown here, but as it is an empirical approach, predictive capabilities would continue to
424 be limited. However, we used MODIS instead as it has a longer coverage for model
425 validation and overlap with the Globe-LFMC data set. It is worth noting that recent
426 developments in the field of remote sensed Vegetation Optical Depth to detect vegetation
427 response to water stress, also allow for enhanced realism in LFMC predictions (Rao et
428 al., 2020). Understanding the potential for high resolution satellites remote sensed
429 Vegetation Optical Depth approaches in monitoring species-specific variations in LFMC
430 is another topic for future development.

431 Despite the large amount of input data required to run MEDFATE simulations
432 (Table A1), much of the complexities of state variables and parameters can be hidden
433 from the user in practical operational tools. Our approach can be implemented within
434 large scale fire danger forecast systems and may pave the way for a new generation of
435 process-based models that are used for operational purposes within fire prevention
436 scenarios.

5. Conclusions

We have developed an approach to predict LFMC by combining a process-based model for the estimation of Ψ_{pd} and an empirical relationship between Ψ_{pd} and LFMC that allows predictions of species-specific seasonal changes and forecasts of future flammability conditions. Our predictions show better agreement with observed LFMC than drought indices or vegetation indices, not only in general terms, but also by species functional types and genus. Our approach can be implemented within large scale fire danger forecast systems and may pave the way for a new generation of process-based models that are used for operational purposes within fire prevention scenarios. As moisture is a critical driver of fire behaviour and considering the projected increases in extreme fire weather events, we suggest the incorporation of plant physiological traits and process-based eco-hydrological models to better constrain fire behaviour projections, and also to better understand fuel availability dynamics for improving fire prevention actions.

Funding: This work was partly founded by the Spanish Government, grant number RTI2018-094691-B-C31 (MCIU/AEI/FEDER, EU). R.B-R. acknowledges the Community of Madrid for the predoctoral contract PEJD-2019-PRE/AMB-15644 funded by the Youth Employment Initiative (YEI). M. De C. was supported by the Spanish Ministry of Science and Innovation via competitive grant CGL2017-89149-C2-2-R. UNED founding for open access publishing.

References

Alberdi, I., Sandoval, V., Condes, S., Cañellas, I., Vallejo, R., 2016. The Spanish

National Forest Inventory, a tool for the knowledge, management and conservation of forest ecosystems. Ecosistemas 25, 88–97. https://doi.org/10.7818/ecos.2016.25-3.10

Balaguer-Romano, R., Díaz-Sierra, R., Madrigal, J., Voltas, J., de Dios, V.R., 2020. Needle senescence affects fire behavior in aleppo pine (Pinus halepensis mill.) stands: A simulation study. Forests. https://doi.org/10.3390/f11101054

Boer, M.M., De Dios, V.R., Stefaniak, E.Z., Bradstock, R.A., 2021. A hydroclimatic model for the distribution of fire on earth. Environ. Res. Commun. 3. https://doi.org/10.1088/2515-7620/abec1f

Borchers-Arriagada, N., Bowman, D.M.J.S., Price, O., Palmer, A.J., Samson, S., Clarke, H., Sepulveda, G., Johnston, F.H., 2021. Smoke health costs and the calculus for wildfires fuel management: a modelling study. Lancet Planet. Heal. 5, e608–e619. https://doi.org/10.1016/s2542-5196(21)00198-4

Cabon, A., Martínez-Vilalta, J., Martínez de Aragón, J., Poyatos, R., De Cáceres, M., 2018. Applying the eco-hydrological equilibrium hypothesis to model root distribution in water-limited forests. Ecohydrology 11. https://doi.org/10.1002/eco.2015

Chakroun, H., Mouillot, F., Hamdi, A., 2015. Regional Equivalent Water Thickness Modeling from Remote Sensing across a Tree Cover/LAI Gradient in Mediterranean Forests of Northern Tunisia 1937–1961. https://doi.org/10.3390/rs70201937

Chazarra Bernabé, A., Flórez García, E., Peraza Sánchez, B., Tohá Rebull, T., Lorenzo Mariño, B., Criado Pinto, E., Moreno García, J.V., Romero Fresneda, R., Botey Fullat, R., 2018. Mapas climáticos de España (1981-2010) y ETo (1996-2016),

Mapas climáticos de España (1981-2010) y ETo (1996-2016). Agencia Estatal de Meteorología. https://doi.org/10.31978/014-18-004-2

Davidson, R., MacKinnon, J., 1993. Estimation and Inference in Econometrics. New York.

De Cáceres, M., Martin-StPaul, N., Turco, M., Cabon, A., Granda, V., 2018. Estimating daily meteorological data and downscaling climate models over landscapes. Environ. Model. Softw. 108, 186–196. https://doi.org/10.1016/j.envsoft.2018.08.003

De Cáceres, M., Martínez-Vilalta, J., Coll, L., Llorens, P., Casals, P., Poyatos, R., Pausas, J.G., Brotons, L., 2015. Coupling a water balance model with forest inventory data to predict drought stress: The role of forest structural changes vs. climate changes. Agric. For. Meteorol. 213, 77–90. https://doi.org/10.1016/j.agrformet.2015.06.012

De Cáceres, M., Mencuccini, M., Martin-StPaul, N., Limousin, J.M., Coll, L., Poyatos, R., Cabon, A., Granda, V., Forner, A., Valladares, F., Martínez-Vilalta, J., 2021. Unravelling the effect of species mixing on water use and drought stress in Mediterranean forests: A modelling approach. Agric. For. Meteorol. 296. https://doi.org/10.1016/j.agrformet.2020.108233

Dinerstein, E., Olson, D., Joshi, A., Vynne, C., Burgess, N.D., Wikramanayake, E., Hahn, N., Palminteri, S., Hedao, P., Noss, R., Hansen, M., Locke, H., Ellis, E.C., Jones, B., Barber, C.V., Hayes, R., Kormos, C., Martin, V., Crist, E., Sechrest, W., Price, L., Baillie, J.E.M., Weeden, D., Suckling, K., Davis, C., Sizer, N., Moore, R., Thau, D., Birch, T., Potapov, P., Turubanova, S., Tyukavina, A., De Souza, N., Pintea, L., Brito, J.C., Llewellyn, O.A., Miller, A.G., Patzelt, A., Ghazanfar, S.A.,

509 Timberlake, J., Klöser, H., Shennan-Farpón, Y., Kindt, R., Lillesø, J.P.B., Van
510 Breugel, P., Graudal, L., Voge, M., Al-Shammari, K.F., Saleem, M., 2017. An
511 Ecoregion-Based Approach to Protecting Half the Terrestrial Realm. Bioscience
512 67, 534–545. https://doi.org/10.1093/biosci/bix014

513 Duane, A., Castellnou, M., Brotons, L., 2021. Towards a comprehensive look at global
514 drivers of novel extreme wildfire events. Clim. Change 165, 1–21.
515 https://doi.org/10.1007/s10584-021-03066-4

516 Gabriel, E., Delgado-Dávila, R., De Cáceres, M., Casals, P., Tudela, A., Castro, X.,
517 2021. Live fuel moisture content time series in Catalonia since 1998. Ann. For.
518 Sci. 78. https://doi.org/10.1007/s13595-021-01057-0

519 Granier, A., Bréda, N., Biron, P., Villette, S., 1999. A lumped water balance model to
520 evaluate duration and intensity of drought constraints in forest stands. Ecol.
521 Modell. 116, 269–283. https://doi.org/10.1016/S0304-3800(98)00205-1

522 Hengl, T., Jesus, J.M. De, Heuvelink, G.B.M., Ruiperez, M., Kilibarda, M., Blagoti, A.,
523 Shangguan, W., Wright, M.N., Geng, X., Bauer-marschallinger, B., Guevara,
524 M.A., Vargas, R., Macmillan, R.A., Batjes, N.H., Leenaars, J.G.B., Ribeiro, E.,
525 Wheeler, I., Mantel, S., Kempen, B., 2017. SoilGrids250m : Global gridded soil
526 information based on machine learning.
527 https://doi.org/10.1371/journal.pone.0169748

528 Hersbach, H., Bell, B., Berrisford, P., Hirahara, S., Horányi, A., Muñoz-Sabater, J.,
529 Nicolas, J., Peubey, C., Radu, R., Schepers, D., Simmons, A., Soci, C., Abdalla, S.,
530 Abellan, X., Balsamo, G., Bechtold, P., Biavati, G., Bidlot, J., Bonavita, M., De
531 Chiara, G., Dahlgren, P., Dee, D., Diamantakis, M., Dragani, R., Flemming, J.,
532 Forbes, R., Fuentes, M., Geer, A., Haimberger, L., Healy, S., Hogan, R.J., Hólm,

E., Janisková, M., Keeley, S., Laloyaux, P., Lopez, P., Lupu, C., Radnoti, G., de Rosnay, P., Rozum, I., Vamborg, F., Villaume, S., Thépaut, J.N., 2020. The ERA5 global reanalysis. Q. J. R. Meteorol. Soc. 146, 1999–2049. https://doi.org/10.1002/qj.3803

IPCC, 2021. Climate Change 2021: The Physical Science Basis. Contribution of Working Group I to the Sixth Assessment Report of the Intergovernmental Panel on Climate Change. Cambridge University Press.

Jolliff, J.K., Kindle, J.C., Shulman, I., Penta, B., Friedrichs, M.A.M., Helber, R., Arnone, R.A., 2009. Summary diagrams for coupled hydrodynamic-ecosystem model skill assessment. J. Mar. Syst. 76, 64–82. https://doi.org/10.1016/j.jmarsys.2008.05.014

Jolly, W.M., Hadlow, A.M., Huguet, K., 2014. De-coupling seasonal changes in water content and dry matter to predict live conifer foliar moisture content. Int. J. Wildl. Fire 23, 480–489. https://doi.org/10.1071/WF13127

Jurdao, S., Chuvieco, E., Arevalillo, J.M., 2012. Modelling fire ignition probability fromsatellite estimates of live fuel moisture content. Fire Ecol. 8, 77–97. https://doi.org/10.4996/fireecology.0801077

Karavani, A., Boer, M.M., Baudena, M., Colinas, C., Díaz-Sierra, R., Pemán, J., de Luis, M., Enríquez-de-Salamanca, Á., Resco de Dios, V., 2018. Fire-induced deforestation in drought-prone Mediterranean forests: drivers and unknowns from leaves to communities. Ecol. Monogr. 88, 141–169. https://doi.org/10.1002/ecm.1285

Luo, K., Quan, X., He, B., Yebra, M., 2019. Effects of live fuel moisture content on wildfire occurrence in fire-prone regions over southwest China. Forests 10, 1–17.

https://doi.org/10.3390/f10100887

Ma, W., Zhai, L., Pivovaroff, A., Shuman, J., Buotte, P., Ding, J., Christoffersen, B., Knox, R., Moritz, M., Fisher, R.A., Koven, C.D., Kueppers, L., Xu, C., 2021. Assessing climate change impacts on live fuel moisture and wildfire risk using a hydrodynamic vegetation model. Biogeosciences 18, 4005–4020. https://doi.org/10.5194/bg-18-4005-2021

Marino, E., Yebra, M., Guill, M., Algeet, N., Tom, L., Madrigal, J., Guijarro, M., Hernando, C., 2020. Investigating Live Fuel Moisture Content Estimation in Fire-Prone Shrubland from Remote Sensing Using Empirical Modelling and RTM Simulations. Remote Sens. 12.

Matthews, S., 2014. Dead fuel moisture research: 1991-2012. Int. J. Wildl. Fire 23, 78–92. https://doi.org/10.1071/WF13005

McDonald, M., 2020. After the fires? Climate change and security in Australia. Aust. J. Polit. Sci. 56, 1–18. https://doi.org/10.1080/10361146.2020.1776680

Moreno-Gutiérrez, C., Barberá, G.G., Nicolás, E., De Luis, M., Castillo, V.M., Martínez-Fernández, F., Querejeta, J.I., 2011. Leaf δ18O of remaining trees is affected by thinning intensity in a semiarid pine forest. Plant, Cell Environ. 34, 1009–1019. https://doi.org/10.1111/j.1365-3040.2011.02300.x

Mouillot, F., Rambal, S., Lavorel, S., 2001. A generic process-based simulator for meditERRanean landscApes (SIERRA): Design and validation exercises. For. Ecol. Manage. 147, 75–97. https://doi.org/10.1016/S0378-1127(00)00432-1

Nolan, R.H., Blackman, C.J., Dios, R. De, Choat, B., Medlyn, B.E., Li, X., Bradstock, R.A., Boer, M.M., 2020. Linking Forest Flammability and Plant Vulnerability to Drought. Forests 1–16.